EUROPEAN ORGANISATION FOR NUCLEAR RESEARCH

CERN-EP/90-94
June 29, 1990

A Study of Coherence of Soft Gluons in Hadron Jets

The OPAL Collaboration [1]

Abstract

We study the inclusive momentum distribution of charged particles in multihadronic events produced in e^+e^- annihilations at $E_{cm} \sim M(Z^0)$. We find agreement with the analytical formulae for gluon production that include the phenomena of soft gluon interference. Using data from c.m. energies between 14 GeV and 91 GeV, we study the dependence of the inclusive momentum distribution on the centre of momentum energy. We find that the analytical formulae describe the data over the entire energy range . Both the momentum distribution at a fixed energy and the change with energy are described by QCD shower Monte Carlos which include either coherent gluon branchings or string fragmentation. Simple incoherent models with independent fragmentation fail to reproduce the energy dependence and momentum spectra.

(submitted to Physics Letters B)

[1] See the following pages for list of authors.

The OPAL Collaboration

M.Z. Akrawy[11], G. Alexander[21], J. Allison[14], P.P. Allport[5], K.J. Anderson[8], J.C. Armitage[6], G.T.J. Arnison[18], P. Ashton[14], G. Azuelos[16,f], J.T.M. Baines[14], A.H. Ball[15], J. Banks[14], G.J. Barker[11], R.J. Barlow[14], J.R. Batley[5], J. Becker[9], T. Behnke[7], K.W. Bell[18], G. Bella[21], S. Bethke[10], O. Biebel[3], U. Binder[9], I.J. Bloodworth[1], P. Bock[10], H. Breuker[7], R.M. Brown[18], R. Brun[7], A. Buijs[7], H.J. Burckhart[7], P. Capiluppi[2], R.K. Carnegie[6], A.A. Carter[11], J.R. Carter[5], C.Y. Chang[15], D.G. Charlton[7], J.T.M. Chrin[14], P.E.L. Clarke[23], I. Cohen[21], W.J. Collins[5], J.E. Conboy[13], M. Couch[1], M. Coupland[12], M. Cuffiani[2], S. Dado[20], G.M. Dallavalle[2], P. Debu[19], M.M. Deninno[2], A. Dieckmann[10], M. Dittmar[4], M.S. Dixit[17], E. Duchovni[24], I.P. Duerdoth[7,d], D.J.P. Dumas[6], H. El Mamouni[16], P.A. Elcombe[5], P.G. Estabrooks[6], E. Etzion[21], F. Fabbri[2], P. Farthouat[19], H.M. Fischer[3], D.G. Fong[15], M.T. French[18], C. Fukunaga[22], A. Gaidot[19], O. Ganel[21], J.W. Gary[10], J. Gascon[16], N.I. Geddes[18], C.N.P. Gee[18], C. Geich-Gimbel[3], S.W. Gensler[8], F.X. Gentit[19], G. Giacomelli[2], V. Gibson[5], W.R. Gibson[11], J.D. Gillies[18], J. Goldberg[20], M.J. Goodrick[5], W. Gorn[4], D. Granite[20], E. Gross[24], J. Grunhaus[21], H. Hagedorn[9], J. Hagemann[7], M. Hansroul[7], C.K. Hargrove[17], I. Harrus[20], J. Hart[5], P.M. Hattersley[1], M. Hauschild[7], C.M. Hawkes[7], E. Heflin[4], R.J. Hemingway[6], R.D. Heuer[7], J.C. Hill[5], S.J. Hillier[1], C. Ho[4], J.D. Hobbs[8], P.R. Hobson[23], D. Hochman[24], B. Holl[7], R.J. Homer[1], S.R. Hou[15], C.P. Howarth[13], R.E. Hughes-Jones[14], R. Humbert[9], P. Igo-Kemenes[10], H. Ihssen[10], D.C. Imrie[23], A. Jawahery[15], P.W. Jeffreys[18], H. Jeremie[16], M. Jimack[7], M. Jobes[1], R.W.L. Jones[11], P. Jovanovic[1], D. Karlen[6], K. Kawagoe[22], T. Kawamoto[22], R.G. Kellogg[15], B.W. Kennedy[13], C. Kleinwort[7], D.E. Klem[17], G. Knop[3], T. Kobayashi[22], T.P. Kokott[3], L. Köpke[7], R. Kowalewski[6], H. Kreutzmann[3], J. Kroll[8], M. Kuwano[22], P. Kyberd[11], G.D. Lafferty[14], F. Lamarche[16], W.J. Larson[4], J.G. Layter[4], P. Le Du[19], P. Leblanc[16], A.M. Lee[15], M.H. Lehto[13], D. Lellouch[7], P. Lennert[10], L. Lessard[16], L. Levinson[24], S.L. Lloyd[11], F.K. Loebinger[11], J.M. Lorah[15], B. Lorazo[16], M.J. Losty[17], J. Ludwig[9], J. Ma[4,b], A.A. Macbeth[14], M. Mannelli[7], S. Marcellini[2], G. Maringer[3], A.J. Martin[11], J.P. Martin[16], T. Mashimo[22], P. Mättig[7], U. Maur[3], T.J. McMahon[1], J.R. McNutt[23], A.C. McPherson[6,c], F. Meijers[7], D. Menszner[10], F.S. Merritt[8], H. Mes[17], A. Michelini[7], R.P. Middleton[18], G. Mikenberg[24], D.J. Miller[13], C. Milstene[21], M. Minowa[22], W. Mohr[9], A. Montanari[2], T. Mori[22], M.W. Moss[14], P.G. Murphy[14], W.J. Murray[5], B. Nellen[3], H.H. Nguyen[8], M. Nozaki[22], A.J.P. O'Dowd[14], S.W. O'Neale[7,e], B.P. O'Neill[4], F.G. Oakham[17], F. Odorici[2], M. Ogg[6], H. Oh[4], M.J. Oreglia[8], S. Orito[22], J.P. Pansart[19], G.N. Patrick[18], S.J. Pawley[14], P. Pfister[9], J.E. Pilcher[8], J.L. Pinfold[24], D.E. Plane[7], B. Poli[2], A. Pouladdej[6], T.W. Pritchard[11], G. Quast[7], J. Raab[7], M.W. Redmond[8], D.L. Rees[1], M. Regimbald[16], K. Riles[1], C.M. Roach[5], S.A. Robins[11], A. Rollnik[3], J.M. Roney[8], S. Rossberg[9], A.M. Rossi[2,a], P. Routenburg[6], K. Runge[9], O. Runolfsson[7], S. Sanghera[6], R.A. Sansum[18], M. Sasaki[22], B.J. Saunders[18], A.D. Schaile[9], O. Schaile[9], W. Schappert[6], P. Scharff-Hansen[7], S. Schreiber[3], J. Schwarz[9], A. Shapira[21], B.C. Shen[4], P. Sherwood[13], A. Simon[3], P. Singh[11], G.P. Siroli[2], A. Skuja[15], A.M. Smith[7], T.J. Smith[1], G.A. Snow[15], R.W. Springer[15], M. Sproston[18], K. Stephens[14], H.E. Stier[9], R. Strohmer[10], D. Strom[8], H. Takeda[22], T. Takeshita[22], T. Tsukamoto[22], M.F. Turner[5], G. Tysarczyk-Niemeyer[10], D. Van den plas[16], G.J. VanDalen[4], G. Vasseur[19], C.J. Virtue[17], H. von der Schmitt[10], J. von Krogh[10], A. Wagner[10], C. Wahl[9], C.P. Ward[5], D.R. Ward[5], J. Waterhouse[6], P.M. Watkins[1], A.T. Watson[1], N.K. Watson[1], M. Weber[10], S. Weisz[7], P.S. Wells[7], N. Wermes[10], M. Weymann[7], G.W. Wilson[19], J.A. Wilson[1], I. Wingerter[7], V-H. Winterer[9], N.C. Wood[13], S. Wotton[7], B. Wuensch[3], T.R. Wyatt[11], R. Yaari[24], Y. Yang[4,b], G. Yekutieli[24], T. Yoshida[22], W. Zeuner[7], G.T. Zorn[15].

[1]School of Physics and Space Research, University of Birmingham, Birmingham, B15 2TT, UK
[2]Dipartimento di Fisica dell' Università di Bologna and INFN, Bologna, 40126, Italy
[3]Physikalisches Institut, Universität Bonn, D-5300 Bonn 1, FRG

[4]Department of Physics, University of California, Riverside, CA 92521 USA
[5]Cavendish Laboratory, Cambridge, CB3 0HE, UK
[6]Carleton University, Dept of Physics, Colonel By Drive, Ottawa, Ontario K1S 5B6, Canada
[7]CERN, European Organisation for Particle Physics, 1211 Geneva 23, Switzerland
[8]Enrico Fermi Institute and Department of Physics, University of Chicago, Chicago Illinois 60637, USA
[9]Fakultät für Physik, Albert Ludwigs Universität, D-7800 Freiburg, FRG
[10]Physikalisches Institut, Universität Heidelberg, Heidelberg, FRG
[11]Queen Mary and Westfield College, University of London, London, E1 4NS, UK
[12]Birkbeck College, London, WC1E 7HV, UK
[13]University College London, London, WC1E 6BT, UK
[14]Department of Physics, Schuster Laboratory, The University, Manchester, M13 9PL, UK
[15]Department of Physics and Astronomy, University of Maryland, College Park, Maryland 20742, USA
[16]Laboratoire de Physique Nucléaire, Université de Montréal, Montréal, Quebec, H3C 3J7, Canada
[17]National Research Council of Canada, Herzberg Institute of Astrophysics, Ottawa, Ontario K1A 0R6, Canada
[18]Rutherford Appleton Laboratory, Chilton, Didcot, Oxfordshire, OX11 0QX, UK
[19]DPhPE, CEN Saclay, F-91191 Gif-sur-Yvette, France
[20]Department of Physics, Technion-Israel Institute of Technology, Haifa 32000, Israel
[21]Department of Physics and Astronomy, Tel Aviv University, Tel Aviv 69978, Israel
[22]International Centre for Elementary Particle Physics and Dept of Physics, University of Tokyo, Tokyo 113, and Kobe University, Kobe 657, Japan
[23]Brunel University, Uxbridge, Middlesex, UB8 3PH UK
[24]Nuclear Physics Department, Weizmann Institute of Science, Rehovot, 76100, Israel

[a]Present address: Dipartimento di Fisica, Università della Calabria, 87036 Rende, Italy
[b]On leave from Harbin Institute of Technology, Harbin, China
[c]Now at Applied Silicon Inc
[d]On leave from Manchester University
[e]On leave from Birmingham University
[f]and TRIUMF, Vancouver, Canada

1 Introduction

We report here on a search for the manifestation of soft gluon coherence in inclusive momentum distributions, predicted by perturbative QCD in the region of low Q^2 [1]. Tests of QCD in e^+e^- collisions have generally been based on measurements of the total hadronic cross section or of quantities such as jet production rates which are related to the high Q^2 behaviour of the theory. Predictions for multiparton distributions at lower Q^2 exist, but these must be related to final state hadron distributions to allow comparison with experiment. In this paper we will directly compare the measured distribution of charged hadron momenta at centre of momentum energy $E_{cm} = M(Z^0)$ with the prediction of QCD. To study the dependence on E_{cm}, we include data taken at lower c.m. energies [2].

In the leading log approximation (LLA) of QCD, both the gluon multiplicity and the shape of the spectrum are predicted with only a scale as a free parameter. The influence of coherence, which is a natural consequence of the quantum mechanical nature of QCD, reduces the available phase space for soft gluon emission to an angular ordered region due to destructive interference. This leads to a slower rise in the gluon multiplicity within a parton jet and to a change in the shape of the gluon momentum distribution relative to the case of incoherence. Coherence also results in an approximately Gaussian distribution of $\ln(1/x)$, where $x = 2E/E_{cm}$, with the maximum asymptotically around $\ln(1/x_0) \approx 0.5\ln(E_{cm}/2\Lambda_{eff})$ in e^+e^- reactions. Here Λ_{eff} is an effective QCD scale, which is not directly related to the usual scale parameters like $\Lambda_{\overline{MS}}$. Once Λ_{eff} is fixed, the evolution of the position of the peak with E_{cm} is unambiguously predicted.

Agreement with coherence predictions has already been found at lower energies in the particle and energy flow distributions of three jet events [3] and in the shape of the $\ln(1/x_p)$ distribution [4]. At Z^0 energies, where the peak of the $\ln(1/x_p)$ distribution is shifted to higher values, phase space constraints are smaller and the low x_p behaviour of the distribution provides a test of the QCD predictions (see discussion in [5]). In addition, a comparison of the $\ln(1/x_p)$ distributions at the Z^0 with those observed at lower energies allows the E_{cm} dependence of the maximum to be tested.

The multiparton momentum spectrum, calculated using perturbative QCD, must be related to the final state hadron distribution to allow for a comparison between theory and experiment. We assume that the calculated gluon spectrum can directly be compared to the measured hadron spectrum, implying that hadronization has only a small effect on the spectrum. This procedure is supported by the concept of Local Parton Hadron Duality (LPHD) [6]. Since the transformation of partons into hadrons should be independent of the c.m. energy, the analysis of the evolution of the hadron spectrum with E_{cm} should be less sensitive to hadronization effects and provide information on the energy evolution of the underlying gluon spectrum. We also compare the measured spectra with the predictions of QCD parton shower Monte Carlo programs which contain detailed models of hadronization and include mass effects and resonance decays.

2 The OPAL Detector and Event Selection

This analysis is based on an integrated luminosity of about 1.3 pb^{-1} collected with the OPAL detector [7] at the e^+e^- collider LEP. The data were recorded at c.m. energies between 88.28 and 95.04 GeV, around the Z^0 pole.

Charged particles were measured with the jet chamber, which is positioned inside a homogeneous magnetic field of 4.3 kG. The magnet coil is surrounded by a time-of-flight counter array and a

lead glass electromagnetic calorimeter. These detectors provided the basic triggers for multihadronic events [8]. The cylindrical jet chamber, which is four metres in length and about two metres in radius, provides a measurement of the momenta of charged particles. Each particle track is measured by up to 159 layers of wires at radii in the range 25.5 cm to 184.5 cm from the beam axis. The single hit resolution is measured to be 140 μm in the plane transverse to the beam (R-ϕ) and 6.0 cm along the direction of the beam (z). The double hit resolution has been determined to 3 mm in the $R-\phi$ plane. The trackfinding efficiency is close to 100 %.

Multihadronic events were preselected using the electromagnetic calorimeter and the time-of-flight counters [8]. The events used in this analysis had to fulfill additional requirements based on jet chamber information to insure that the events were well contained within the sensitive volume: Multihadronic events were required to have at least five well measured tracks. A well measured track was reconstructed from at least 40 hits in the jet chamber (corresponding to an effective cut $|\cos(\theta)| \leq 0.92$), had to have a minimum transverse momentum to the beam axis of 200 MeV/c and a reconstructed distance of closest approach to the beam axis of less than 5 cm. The energy sum of all accepted tracks had to exceed 5 GeV. The absolute value of the cosine of the angle between the thrust axis and the beam axis was required to be smaller than 0.86. A total of 22959 events satisfied these requirements.

3 The Particle Momentum Spectrum at $E_{cm} = M(Z^0)$

In fig.1 we display the inclusive momentum distribution of charged particles in terms of $\ln(1/x_p)$ with $x_p = (2 \cdot p/E_{cm})$, p being the momentum of each hadron. The distribution is corrected for detector acceptance and resolution effects and for initial state radiation. The correction procedure is based on a detailed Monte Carlo simulation of the OPAL detector and is described in [9]. It leads to x_p dependent correction factors

$$c(x_p) \;=\; \left(\frac{n_{gen}(x_p)}{N_{gen}}\right) / \left(\frac{n_{rec}(x_p)}{N_{rec}}\right)$$

where $n(x_p)$ denotes the number of tracks with scaled momentum x_p and N the number of Monte Carlo events considered. The indices 'gen' and 'rec' refer to the generated and reconstructed yields. We restrict the analysis to the region of $0.20 \leq p \leq 45$ GeV/c, corresponding to $0 \leq \ln(1/x_p) \leq 5.4$. Throughout this region, the correction is everywhere less than 20%.

Various checks have been performed to estimate possible uncertainties in the correction procedure and in the representation of the detector by the Monte Carlo program. In particular we investigated possible effects on the shape of the $\ln(1/x_p)$ distribution.

- The binning in $\ln(1/x_p)$ was adjusted such that the migration between bins due to resolution effects was below ≈ 5 %.
- We varied parameters in the simulation describing the detector performance: The accuracy of the hit position in z was varied in the range between 6 and 30 cm, the resolution in the r- ϕ plane from 120 to 160 μm, and the double hit resolution from 2 to 3 mm. The correction factors did not vary by more than 3%, which is the same size as the statistical errors for these Monte Carlo simulations.
- Parameters in the track finding program were varied to estimate the effect of possible differences between Monte Carlo and data. For reasonable parameter changes the variation of the correction factors was less than 5%. Since this effect was momentum independent, the shape of the $\ln(1/x_p)$ distribution was not affected.

- The correction factors were determined with different QCD Monte Carlos [10,11]. No difference within the statistical precision was observed. The uncertainty of the correction factors due to hadronization is at most 0.5%.
- We looked at subsamples of tracks in different regions of the polar angle with respect to the beam axis and separately for positively and negatively charged tracks. The data agreed with the Monte Carlo expectation for the same cuts within 3%.

In total we assign a 5% systematic error to the absolute normalization. The more important relative systematic error between different values of x_p is much smaller than 5%.

In fig.1 the measured corrected $\ln(1/x_p)$ distribution of charged particles in hadronic events at $E_{cm} = M(Z^0)$ is shown. It has a broad maximum around $\ln(1/x_0) \approx 3.6$. The decrease towards high x_p (low $\ln(1/x_p)$) values reflects energy and momentum conservation. The measured particle yield is listed in table 1 as a function of $\ln(1/x_p)$. The errors displayed are statistical only.

To perform fits to the observed spectrum, we used theoretical formulae for gluons that differ in the treatment of terms beyond the next to leading order in the QCD calculations. These calculations are valid for relativistic particles in a region not too far from the peak of the $\ln(1/x)$ distribution.

First we use the modified leading log approximation (MLLA) [12] which takes into account all leading and next to leading logarithmic terms. The MLLA predicts a spectrum of the form

$$\frac{1}{\sigma}\frac{d\sigma}{d\ln(1/x)} = \frac{4N_c}{b}\Gamma(B)K(Y)\int_{a_0-i\frac{\pi}{2}}^{a_0+i\frac{\pi}{2}}\frac{d\tau}{\pi}e^{-B\alpha}\left[\frac{C(\alpha,\ln(1/x),Y)}{\frac{4N_c}{b}Y\frac{\alpha}{\sinh\alpha}}\right]^{\frac{B}{2}} I_B\left(\sqrt{D(\alpha,\ln(1/x),Y)}\right) \quad (1)$$

for the $\ln(1/x)$ distribution. Here

$$D(\alpha,\ln(1/x),Y) = \frac{16N_c}{b}Y\frac{\alpha}{\sinh\alpha}C(\alpha,\ln(1/x)),$$

$$C(\alpha,\ln(1/x),Y) = \cosh\alpha + \left(\frac{2\ln(1/x)}{Y} - 1\right)\sinh\alpha$$

with $Y = \ln(E_{cm}/2\Lambda_{eff})$ and $\alpha = \alpha_0 + i\tau$. For the integration α_0 was chosen according to $\tanh\alpha_0 = (1 - (2\ln(1/x)/Y))$ [2]; $b = 11N_c/3 - 2N_f/3$ and $B = (11N_c/3 + 2N_f/3/N_c^2)/b$ are defined by the number of flavours N_f and colours N_c. I_B is the modified Bessel function of order B. In this formula, which represents the standard MLLA result for particle spectra [12] [14] in a convenient form for numerical integration, the parton shower evolution and the fragmentation are factorized. The overall normalization factor $K(Y)$ describes the transformation of partons into hadrons. Motivated by LPHD we choose it to depend only on Y. Thus formula (1) has only Λ_{eff} and an overall normalization from $K(Y)$ as free parameters. We performed a numerical integration to fit this formula to our data.

For asymptotic energies E_{cm} and close to the peak, formula (1) can be approximated by a Gaussian distribution [14]

$$\frac{1}{\sigma}\frac{d\sigma}{d\ln(x)} \approx N(Y)\left(\frac{c_1}{\pi Y^{3/2}}\right)^{1/2}\exp\left[\frac{-c_1\left(\ln\frac{1}{x} - \ln\frac{1}{x_0}\right)^2}{Y^{3/2}}\right] \quad (2)$$

with x_0, the position of the maximum, at [14] [15]

$$\ln\frac{1}{x_0} = 0.5\cdot Y + c_2\cdot\sqrt{Y} + O(1) \quad (3)$$

[2] There is a misprint in [12] where $\tan(\alpha_0)$ is given while $\tanh(\alpha_0)$ should be used [13]

and $c_1 = \sqrt{36N_c/b}$, $c_2 = B\sqrt{b/16/N_c}$ constants given by theory. The average multiplicity N(Y) is predicted by theory up to a normalization factor K_G. The second free parameter is Λ_{eff}. The term $O(1)$ contains higher order corrections and should be constant for $E_{cm} \to \infty$.

A second expression for the spectrum results in a Gaussian with higher moments [16]:

$$\frac{1}{\sigma}\frac{d\sigma}{d\ln(x)} \approx \frac{N(Y)}{\sigma\sqrt{2\pi}} \exp\left[\frac{1}{8}k - \frac{1}{2}s\delta - \frac{1}{4}(2+k)\delta^2 + \frac{1}{6}s\delta^3 + \frac{1}{24}k\delta^4\right] \tag{4}$$

with $\delta = (\ln(1/x) - \overline{\ln(1/x)})/\sigma$. $\overline{\ln(1/x)} = \ln(1/x_0) + O(1)$ is the mean value of the distribution. The coefficients $N(Y)$, σ, s and k are the average multiplicity, the width, skewness and kurtosis [16] of the Gaussian like momentum spectrum and are calculated to next-to-leading order. Apart from Λ_{eff} this formula contains an unknown higher order correction term $O(1)$ to $\ln(1/\bar{x})$ as well as yet unknown higher order terms in the parameters σ, s and k. The latter were not taken into account for the analysis in order to limit the number of free parameters.

Fits to the measured charged particle momentum spectrum [3] were performed using formulae (1), (2) and (4). The fits were restricted to the region around the maximum in the interval $2.5 \leq ln(1/x) \leq 4.5$ which corresponds to the region of validity of the analytical formulae. The number of flavours was set to $N_f = 3$, as the three light quark species dominate quark pair production in the gluon cascade. For $N_f = 5$ the data can also be described by the analytical expressions with different values of Λ_{eff} and $O(1)$. In table 2 and fig.1 we display the results of the fits. In all three cases the region around the maximum and the falloff towards low x_p (high $\ln(1/x_p)$), where these formulae are valid, are well described. This agreement of the shape and the peak position of the measured hadron distribution with a formula derived for gluons is consistent with the concept of Local Parton Hadron Duality [6]. While formula (1) and its Gaussian approximation (2) provide a good description of the spectrum over almost the entire x_p range, they under- and overestimate the particle yield in the region of nonrelativistic momenta at small x_p. The expansion (4) of a Gaussian distribution describes the small x_p region very well, but overestimates the particle yield in the region of high x_p.

In fig. 2 we compare our measurement with the results from QCD shower Monte Carlo programs. JETSET 7.2 [10] and HERWIG 3.4 [11] contain the basic features of the QCD parton branching processes including colour coherence. The fragmentation parameters were tuned to describe the global event shapes as measured by OPAL [9]. To test the coherence effect we also used other options in the JETSET program: In a first step, the partons were evolved with incoherent branchings and the string fragmentation was used. Both experimental [3] and theoretical [18] results indicate that string fragmentation reproduces part of the coherence effect. In a second step the string fragmentation was replaced by the independent fragmentation [10]. The fragmentation parameters for the two options based on incoherent parton shower evolution were adjusted to describe the average charged multiplicity and to approximately reproduce the position of the maximum of the $\ln(1/x_p)$ distribution (see fig. 2).

The Monte Carlos based on coherent parton showers give a good description of the observed distribution at $E_{cm} \approx 91\,GeV$. This is also true for the incoherent parton shower option with string fragmentation. The Monte Carlo which combines incoherent parton branchings with independent jet fragmentation predicts a higher maximum and a distribution which decreases faster than the data for $x_p > x_0$.

[3] The QCD formulae are derived for massless gluons and therefore do not discriminate between momentum and energy. The observed hadron momentum and energy spectra are similar for relativistic particles only. Protons for example are not relativistic in the region of the peak of the $\ln(1/x_p)$ distribution at 91 GeV. Since we are dealing with unidentified stable charged particles, we choose the particle momenta for the comparison with the theoretical prediction. In [17] it was pointed out that the particle spectra should be different for different particle types.

4 The energy evolution of the maximum

QCD not only predicts the shape of the gluon momentum distribution at a fixed energy but also describes the energy evolution of the spectrum. Hadronization effects may influence the shape of the measured momentum distribution. If such a distortion is the same at all c.m. energies, the theoretical prediction for the underlying parton distribution can be tested by studying the energy evolution of the $\ln(1/x_p)$ distribution. Concepts like LPHD support such a procedure. Fixing the parameters in formulae (1) to (4) to the values obtained at $E_{cm} = M(Z^0)$ leads to an unambiguous prediction of the theory for other c.m. energies. In the case of the Monte Carlo generators JETSET, HERWIG and ARIADNE [19] it has been shown that energy independent fragmentation parameters lead to a consistent description of global event shape distributions for the energy range between $E_{cm} = 29\,GeV$ and $E_{cm} = 91\,GeV$ [9]. For the following analysis we therefore leave the fragmentation parameters of all Monte Carlo models at the values obtained at $E_{cm} = M(Z^0)$. The energy evolution of the hadron spectrum should then reflect the energy evolution of the underlying parton distribution.

To investigate the energy evolution, we combine our measurement with the results obtained by the TASSO collaboration at c.m. energies between 14 and 44 GeV [2]. We first compare the observed distributions to the analytical formulae (1) and (4) and the QCD Monte Carlos JETSET and HERWIG; next we discuss the variation of the position of the peak of the momentum spectrum with energy.

Figure 3a displays the measurements of the $\ln(1/x_p)$ distributions for c.m. energies between 14 and 91 GeV together with the predictions of the analytical formulae (1) (full line) and (4) (dotted line). The parameters Λ_{eff} and O(1) were fixed to the values which were obtained from the fit to the spectrum at $E_{cm} = M(Z^0)$ (table 2). For the lower c.m. energies, the normalizations $K(Y)$ in (1) and $N(Y)$ in (4) were determined for each energy point separately from a fit to a region of about $\Delta \ln(1/x_p) \approx 1$ around the peak of the lower energy spectra (see also table 3).

From figure 3a it is seen that the height of the maximum rises with increasing energy, reflecting the increase in multiplicity. The position of the maximum $\ln(1/x_0)$ is shifted to larger $\ln(1/x_p)$ values, while the width of the distribution increases only moderately. For high x_p, the slightly lower particle yield with increasing c.m. energies indicates the scaling violations of the fragmentation function.

Due to particle mass effects, the spectra should be similar in the region of small momenta at all c.m. energies. This can be seen in figure 3b, where the $\ln(p)$ distribution is shown. The peak of the distribution at high c.m. energies is separated from the region where the influence of the hadron masses is important.

In the region $p > \Lambda_{eff}$, the theoretical formula (1) describes the TASSO data at all energy points very well, thus demonstrating the consistency of the data with the conjectures of coherence and LPHD. For small momenta, where the particles are nonrelativistic, the falloff in the predicted particle yield tends to be steeper than in the data. In the region of $p < \Lambda_{eff}$ the theoretical formula (1) is not valid. Accordingly, the curves are restricted to the region $p > \Lambda_{eff}$ in figures 3a and 3b. We observe that $K(Y)$ increases with decreasing c.m. energies, possibly indicating the influence of c.m. energy dependent effects in the LPHD- MLLA picture (table 3).

The results obtained for the distorted Gaussian (equ. 4) are also displayed in fig. 3a. The normalization factors are in good agreement with the measured charged particle multiplicities also in the energy range between 14 and 44 GeV (see e.g. [4]). As was already seen for $E_{cm} = 91\,GeV$, the region of small x is well described. However, the height of the peak of the $\ln(1/x_p)$ distribution is underestimated. In the high x_p region, the predicted particle yield is overestimated.

Fig. 3c shows a comparison of the measured charged particle momentum distribution with the predictions from two QCD shower Monte Carlo generators using parameters from an optimization at $E_{cm} = 91\,GeV$ [9]. The Monte Carlos describe the data in the range of high momenta very well for all c.m. energies. At small c.m. energies, both the HERWIG and the JETSET Monte Carlo overestimate the particle yield in the region of the peak of the spectrum and at low momenta.

An essential manifestation of coherence is the energy dependence of the peak position $\ln(1/x_0)$ which QCD predicts to change according to formula (3). Therefore we next compare the observed shift of $\ln(1/x_0)$ with the theoretical predictions and with those from the Monte Carlo programs. To determine the position of the maximum of the distributions, we fitted the spectra at all five energy points to a fifth order polynomial and to a function of the form

$$\frac{1}{\sigma}\frac{d\sigma}{d\ln(1/x)} = F\exp\left(\frac{1}{8}k - \frac{1}{2}sd - \frac{1}{4}(2+k)d^2 + \frac{1}{6}sd^3 + \frac{1}{24}kd^4\right) \qquad (5)$$

with $d = (\ln(1/x) - \ln(1/x_f))/\sigma$. The choice of the fit function (5) was motivated by the analytical spectrum (4). For the fit, the parameters F, x_f, σ, s and k in equation (5) were left free. To avoid systematic uncertainties due to the choice of the bin range and due to the selection of the fit function, we varied the bin range used for the fits and determined the position of the maximum by averaging over all fits. The polynomial fit function is not model dependent and was used to reduce possible systematic uncertainties from the choice of the exponential fit function (5). Both the polynomial and the exponential fit function give the same values for the position of the maximum within the statistical accuracy. At $E_{cm} = M(Z^0)$ we obtain a value of $\ln(1/x_0) = 3.603 \pm 0.013(stat.) \pm 0.040(syst.)$, corresponding to $\ln(p_0) = 0.216 \pm 0.013(stat.) \pm 0.040(syst.)$ or $p_0 = 1.24\,GeV/c$, for the position of the maximum of the $\ln(1/x_p)$- and the $\ln(p)$- distribution, respectively.

The energy evolution of $\ln(1/x_0)$ is displayed in figure 4 together with the QCD prediction $\ln\frac{1}{x_0} = 0.5\cdot Y + c_2\cdot\sqrt{Y} + O(1)$ (equ. 3) for $\Lambda_{eff} = 0.203\ GeV$ and $O(1) = -0.384$, obtained from the fit of equation (2) to the shape of the spectrum at 91 GeV. The agreement with the data is excellent. From a fit to the predicted energy evolution of the position of the maximum we obtain $\Lambda_{eff} = 0.212 \pm 0.020\ GeV$ and $O(1) = -0.321 \pm 0.60$. The value of Λ_{eff} obtained is compatible with the results from the fits of the analytic functions to the data at 91 GeV (table 2). Omission of the term $O(1)$ in (3) can be compensated by a larger value of $\Lambda_{eff} \approx 0.35$ and also gives a good description of the data.

In the c.m. energy range considered, the evolution of the peak position of the $\ln(1/x_p)$ spectrum and equation (3) can be approximated by a straight line (see fig. 4). We therefore use a straight line fit of the form

$$\ln(1/x_0) = b\cdot\ln(E_{cm}) + c \qquad (6)$$

and obtain a slope of $b = 0.637 \pm 0.016$ and an intercept of $c = 0.735 \pm 0.067$. If the spectrum of soft particles in jets were dominated by phase space effects and not by colour coherence, the peak of the $\ln(1/x_p)$ distribution would show a c.m. energy behaviour of $b = 1$. This is in obvious disagreement with the data.

Next we compare the energy evolution of the maximum with that predicted by the Monte Carlo programs discussed above. The advantage of using Monte Carlos is that phase space effects, mass dependences and distortions due to hadronization are explicitly included. The disadvantage is the large variety of possible parameter combinations in the fragmentation part. We leave the fragmentation parameters for all energy points fixed at the values obtained by optimizations at $E_{cm} = 91\ GeV$.

The position of the maximum of the $\ln(1/x_p)$ distribution predicted by Monte Carlo programs as a function of the c.m. energy is shown in fig. 4. Results of straight line fits are listed in table 4. In

addition to the slope determined after hadronization, we also list the slope obtained from distributions of partons generated in the parton shower in table 4. At high energies the parton distribution obtained from the JETSET incoherent parton shower branchings is flat and does not exhibit a pronounced maximum. In this case we therefore used the mean values of $\ln(1/x_p)$ to determine the slope for the parton distributions.

The simulations based on coherent gluon emission are in good agreement with the measurements. Both JETSET and HERWIG yield a slope after hadronization which is larger than the one for the corresponding gluon distribution. The slope obtained from the ARIADNE model is slightly larger than observed in the data. For the case of incoherent gluon branchings in JETSET we find a trend towards steeper energy dependences if string fragmentation is used. In this case, the value for b is 2.8 standard deviations larger than the measurement.

As mentioned before, string fragmentation partly incorporates coherence effects. If string fragmentation for the incoherent parton branching is replaced by independent fragmentation, the energy dependence obtained has a slope of about 1 as is expected from phase space and fails to reproduce the data. The energy variation in this case deviates from a linear increase with $\ln(E_{cm})$ at lower energies (see fig. 4). Restricting the energy range to $E_{cm} \geq 35\ GeV$, we obtain a slope of $b = 1.004 \pm 0.023$, which is consistent with pure phase space. This failure of the independent fragmentation model demonstrates the sensitivity of the measurement to coherence and that the results are not biased by the selection criteria. The results for the independent fragmentation model are rather insensitive to the actual choice of fragmentation parameters as long as they are kept c.m. energy independent. To verify this, we changed the hardness and the transverse component of the fragmentation function over a large range as well as the cutoff parameter Q_0 and the scale parameter Λ_{QCD} in the parton shower. Keeping the charged multiplicity fixed at 91 GeV, the variation Δb of the slope was never greater than 15%.

5 Summary

We have measured the inclusive momentum distribution of charged particles in e^+e^- collisions at the Z^0 energy. We have compared the measured spectrum with theoretical predictions for gluons which include the coherence of soft gluon radiation. After adjusting the overall normalization and effective scale parameter Λ_{eff}, we find that the analytic QCD formulae provide a good description of the momentum distribution at 91 GeV, especially in the region of the peak of the spectrum. Using the value $\Lambda_{eff} = 253\ MeV$ found for 91 GeV, the QCD formulae also describe the inclusive momentum distribution measured at c.m. energies between 14 and 44 GeV. Increasing the c.m. energy from 14 to 91 GeV, the overall normalization factor decreases by 15 %. The good agreement between the QCD formulae for gluons and the measured charged hadron distributions establishes the consistency of the measurements with colour coherence and Local Parton Hadron Duality in e^+e^- hadronic reactions.

One of the manifestations of colour coherence is the existence of a peak in the $\ln(1/x_p)$ distribution. We observe that the evolution of this peak position with E_{cm} is accurately predicted by the analytical formulae.

We also compared the measurement with the prediction from QCD Monte Carlos. Various parton shower models based on coherent and incoherent branchings with appropriately tuned parameters can reproduce the data at fixed $E_{cm} = 91\ GeV$. Fixing the parameters of these models to describe our data, we find the best agreement of the low energy data with models based on coherent gluon emission. Choosing incoherent parton branchings and string fragmentation we find a somewhat worse

description of the energy dependence of the position of the maximum. However an incoherent parton shower model with independent fragmentation is incompatible with the data.

Acknowledgements

We wish to thank Ya.I.Azimov, Yu.L.Dokshitzer, T.Sjöstrand, S.I.Troyan, B.Webber and P.Zerwas for many clarifying and enjoyable discussions. Our special thanks go to V.Khoze for his continuing interest and encouragement.

It is a pleasure to thank the SL Division for the efficient operation of the LEP accelerator, the precise information on the absolute energy, and their continuing close cooperation with our experimental group. In addition to the support staff at our own institutions we are pleased to acknowledge the following :
Department of Energy, USA
National Science Foundation, USA
Science and Engineering Research Council, UK and The A.P. Sloan Foundation.
National Sciences and Engineering Research Council,Canada
Israeli Ministry of Science
Minerva Gesellschaft
The Japanese Ministry of Education, Science and Culture (the Monbusho) and a grant under the Monbusho International Science Research Program.
American Israeli Bi-national Science Foundation.
Direction des Sciences de la Matiere, France.
The Bundesministerium für Forschung und Technologie, FRG.

References

[1] A.H.Mueller, Phys.Lett. B104(1981)161; A.Bassetto, M.Ciafaloni, G. Marchesini and A.H.Mueller, Nucl. Phys. B207(1982)189; B.I.Ermolaev and V.S.Fadin, JETP Lett. 33(1981)269; Yu.L.Dokshitzer, V.S.Fadin, V.A.Khoze, Phys. Lett. B115(1982)242

[2] TASSO collaboration, W.Braunschweig et al., DESY 90-013

[3] JADE collaboration, W.Bartel et al., Phys.Lett B134(1985)31; TPC collaboration, H.Aihara et al., Z.Phys. C28(1985)31; TPC collaboration, Phys. Rev. Lett. 57(1986)945

[4] TASSO collaboration, M.Althoff et al., Z.Phys. C22(1984)307; HRS collaboration, D.Bender et al., Phys. Rev. D31(1985)1; TPC collaboration, H.Aihara et al., Phys. Rev. Lett. 52(1984)577

[5] P.Mättig, Phys. Rep. 177(1989)141

[6] D.Amati and G.Veneziano, Phys.Lett B83(1979)87; Ya.I.Azimov, Yu.L.Dokshitzer, V.A.Khoze and S.I.Troyan, Z.Phys C27(1985)65

[7] OPAL Technical proposal (1983) and CERN LEPC/83-4; OPAL Collaboration, K. Ahmet et al., "The OPAL detector at LEP", to be submitted to Nucl. Instr. and Meth.

[8] OPAL collaboration, M.Z.Akrawy et al., Phys.Lett 231B(1989)530

[9] OPAL collaboration, M.Z.Akrawy et al., CERN-EP/90-48, to be published in Z. Phys. C

[10] T.Sjöstrand, Comp. Phys. Comm. 39(1986)347 JETSET, Version 7.2; P.Andersson, G.Gustafson, G.Ingelman and T.Sjöstrand, Phys. Rep. 97(1983)33

[11] G.Marchesini and B.R.Webber, Nucl.Phys. B310(1988)461; HERWIG, Version 3.4

[12] Yu.L.Dokshitzer, S.Troyan, Leningrad preprint LNPI No.922 (1984);

[13] Yu.L.Dokshitzer, V.A.Khoze, private communication

[14] Yu.L.Dokshitzer, V.A.Khoze and S.Troyan, in Perturbative Quantum Chromodynamics, ed. A.H.Mueller, World Scientific, Singapore (1989)241; Yu.L.Dokshitzer, V.A.Khoze, A.H.Mueller and S.I.Troyan, Rev.Mod.Phys. 60(1988)373

[15] Yu.L.Dokshitzer, V.A.Khoze, G.Marchesini, B.R. Webber, CERN TH-5738/90 (1990); V.A.Khoze, private communication; B.R.Webber, private communication

[16] C.P.Fong and B.R.Webber, Phys. Lett. B229(1989)289; see also Z.Kunszt et al. in Z Physics at LEP I, ed. G.Altarelli, R.Kleiss and C.Verzegnassi, CERN 89-08, Vol.I

[17] Ya.I.Azimov, Yu.L.Dokshitzer, V.A.Khoze and S.I.Troyan, Z. Phys. C31(1986)213

[18] Y.Azimov et al., Yad.Fiz. 43(1986)149; Phys.Lett. B165(1985)147

[19] G.Gustafson and U. Pettersson, Nucl.Phys. B306(1988)746; U.Pettersson, LU TP 88-5 (1988); L.Lönnblad and U.Pettersson, LU TP 88-15 (1988); L.Lönnblad, LU TP 89-10 (1989)

Tables

Table 1: Differential cross section $1/\sigma\, d\sigma/d\ln(1/x)$ at W = 91 GeV The errors shown are statistical errors only. There is an overall systematic error of 5 %. The bin to bin systematic errors are much smaller than the statistical errors (see text) and are not shown.

ln(1/x)	$1/\sigma\, d\sigma/d\ln(1/x)$	ln(1/x)	$1/\sigma\, d\sigma/d\ln(1/x)$
0.019 – 0.119	0.003 ± 0.001	2.719 – 2.819	5.467 ± 0.082
0.119 – 0.219	0.013 ± 0.002	2.819 – 2.919	5.803 ± 0.084
0.219 – 0.319	0.033 ± 0.004	2.919 – 3.019	5.943 ± 0.084
0.319 – 0.419	0.096 ± 0.01	3.019 – 3.119	6.049 ± 0.084
0.419 – 0.519	0.119 ± 0.009	3.119 – 3.219	6.221 ± 0.086
0.519 – 0.619	0.197 ± 0.014	3.219 – 3.319	6.322 ± 0.086
0.619 – 0.719	0.287 ± 0.016	3.319 – 3.419	6.619 ± 0.091
0.719 – 0.819	0.394 ± 0.02	3.419 – 3.519	6.446 ± 0.088
0.819 – 0.919	0.564 ± 0.025	3.519 – 3.619	6.599 ± 0.09
0.919 – 1.019	0.771 ± 0.031	3.619 – 3.719	6.687 ± 0.089
1.019 – 1.119	0.922 ± 0.032	3.719 – 3.819	6.642 ± 0.089
1.119 – 1.219	1.183 ± 0.038	3.819 – 3.919	6.436 ± 0.086
1.219 – 1.319	1.302 ± 0.037	3.919 – 4.019	6.296 ± 0.085
1.319 – 1.419	1.611 ± 0.044	4.019 – 4.119	6.206 ± 0.084
1.419 – 1.519	1.837 ± 0.045	4.119 – 4.219	5.997 ± 0.082
1.519 – 1.619	2.059 ± 0.048	4.219 – 4.319	5.87 ± 0.083
1.619 – 1.719	2.548 ± 0.058	4.319 – 4.419	5.635 ± 0.082
1.719 – 1.819	2.722 ± 0.057	4.419 – 4.519	5.198 ± 0.078
1.819 – 1.919	3.000 ± 0.059	4.519 – 4.619	4.786 ± 0.073
1.919 – 2.019	3.339 ± 0.063	4.619 – 4.719	4.637 ± 0.075
2.019 – 2.119	3.658 ± 0.067	4.719 – 4.819	4.189 ± 0.071
2.119 – 2.219	3.768 ± 0.065	4.819 – 4.919	3.923 ± 0.071
2.219 – 2.319	4.174 ± 0.071	4.919 – 5.019	3.559 ± 0.068
2.319 – 2.419	4.606 ± 0.075	5.019 – 5.119	3.246 ± 0.071
2.419 – 2.519	4.894 ± 0.08	5.119 – 5.219	2.767 ± 0.066
2.519 – 2.619	4.896 ± 0.077	5.219 – 5.319	2.515 ± 0.074
2.619 – 2.719	5.417 ± 0.082	5.319 – 5.419	2.352 ± 0.091

Table 2: Parameters of the analytical formulae obtained from a fit to our data. K corresponds to the overall normalization factor required for (1) and (2). $N(Y)$ was obtained from fitting formula (4) to the data and agrees well with the charged multiplicity measured by OPAL [9]. The errors shown are the statistical errors of the fit parameters and do not include systematic effects.

Analytic Formula	First Parameter	Second Parameter	Third Parameter	χ^2/df
1	$\Lambda_{eff} = 0.253 \pm 0.030$	$K = 1.28 \pm 0.01$		1.30
2	$\Lambda_{eff} = 0.203 \pm 0.030$	$K_G = 0.19 \pm 0.01$	$O(1) = -0.38 \pm 0.09$	0.97
4	$\Lambda_{eff} = 0.255 \pm 0.026$	$N(Y) = 21.4 \pm 0.3$	$O(1) = -1.00 \pm 0.07$	0.94

Table 3: Normalization factors K(Y) and N(Y) at different c.m. energies

E_{cm}	$K(Y)$	χ^2/df	$N(Y)$	χ^2/df
91 GeV	1.28 ± 0.01	1.3	21.4 ± 0.3	0.9
44 GeV	1.31 ± 0.01	3.4	15.2 ± 0.1	1.8
35 GeV	1.36 ± 0.01	4.9	13.7 ± 0.1	18.0
22 GeV	1.38 ± 0.02	0.7	11.2 ± 0.2	1.4
14 GeV	1.46 ± 0.02	0.6	9.0 ± 0.1	2.2

Table 4: Slopes obtained from various Simulation schemes

Model	Coherence	Fragmentation	slope (partons)	slope (hadrons)
Data				0.637±0.016
MLLA (Equ. 1)	yes		0.627	
HERWIG	yes	cluster	0.600±0.012	0.629±0.036
ARIADNE	yes	string		0.686±0.020
JETSET	yes	string	0.597±0.036	0.663±0.019
	no	string	0.666±0.003	0.692±0.012
	no	independent		0.952±0.017

Figures

Figure 1: $\ln(1/x_p)$ distribution at $E_{cm} = 91\,GeV$ compared with analytical formulae. The measured distribution is compared to the analytical formulae using the parameters in table 2.

Figure 2: $\ln(1/x_p)$ distribution at $E_{cm} = 91\,GeV$ compared with QCD Monte Carlos

Figure 3a: $\ln(1/x_p)$ distributions at E_{cm} = 14, 22, 35, 44 and 91 GeV.

Figure 3b: Ln(p) distributions at E_{cm} = 14, 22, 35, 44 and 91 GeV

Figure 3c: Ln(p) distributions at E_{cm} =14, 22, 35, 44 and 91 GeV compared with QCD Monte Carlos

Figure 4: Energy evolution of the maximum of $ln(1/x_p)$ compared to the analytical formula (3) (full line) and some QCD Monte Carlos.

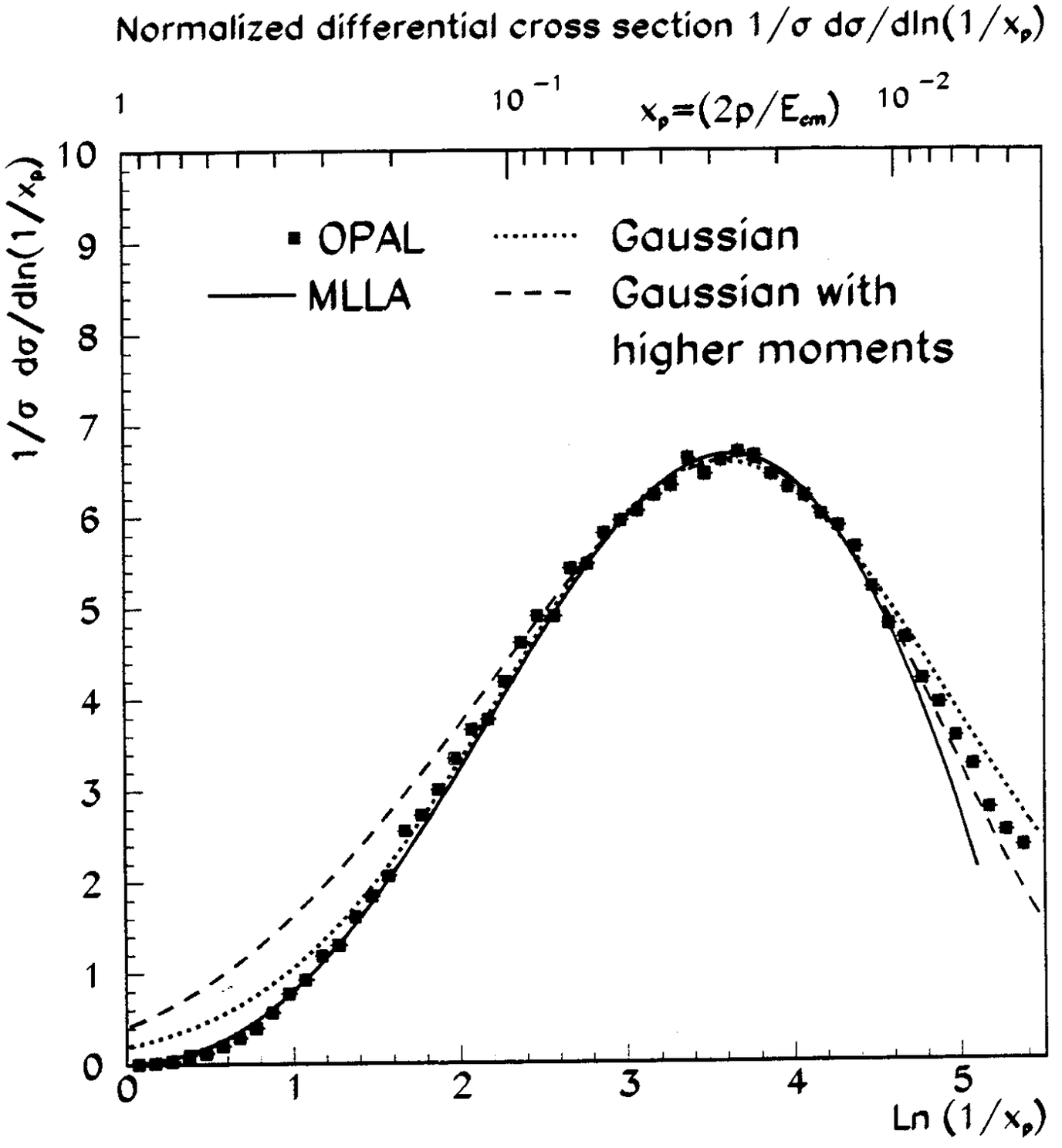
Normalized differential cross section 1/σ dσ/dln(1/x_p)
1
10^-1
x_p=(2p/E_cm)
10^-2
1/σ dσ/dln(1/x_p)
10
9
8
7
6
5
4
3
2
1
0
OPAL
MLLA
Gaussian
Gaussian with higher moments
0
1
2
3
4
5
Ln (1/x_p)

Figure 1

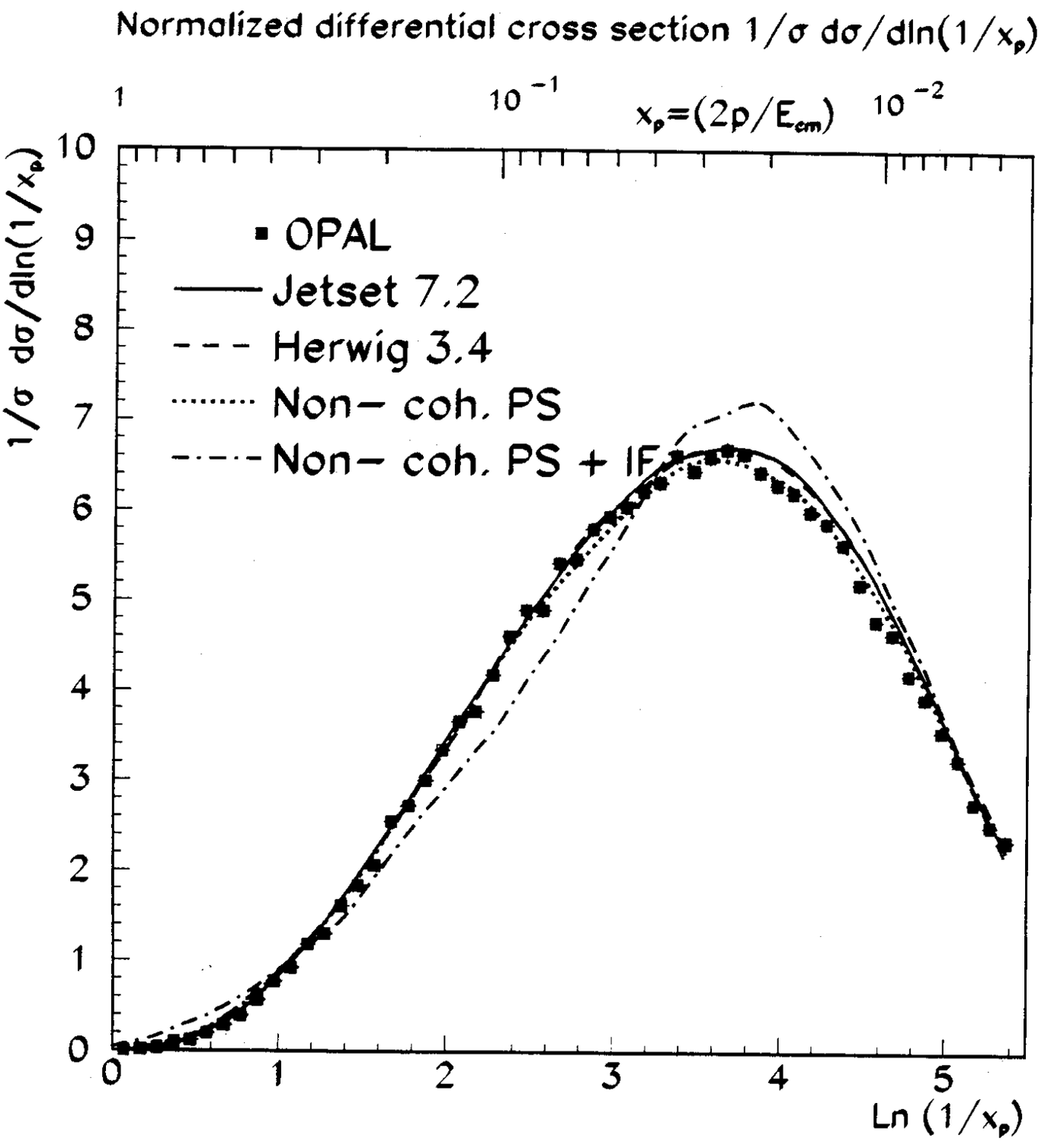
Normalized differential cross section 1/σ dσ/dln(1/x_p)
1
10^-1
x_p=(2p/E_cm)
10^-2
1/σ dσ/dln(1/x_p)
OPAL
Jetset 7.2
Herwig 3.4
Non− coh. PS
Non− coh. PS + IF
Ln (1/x_p)
0
1
2
3
4
5
6
7
8
9
10

Figure 2

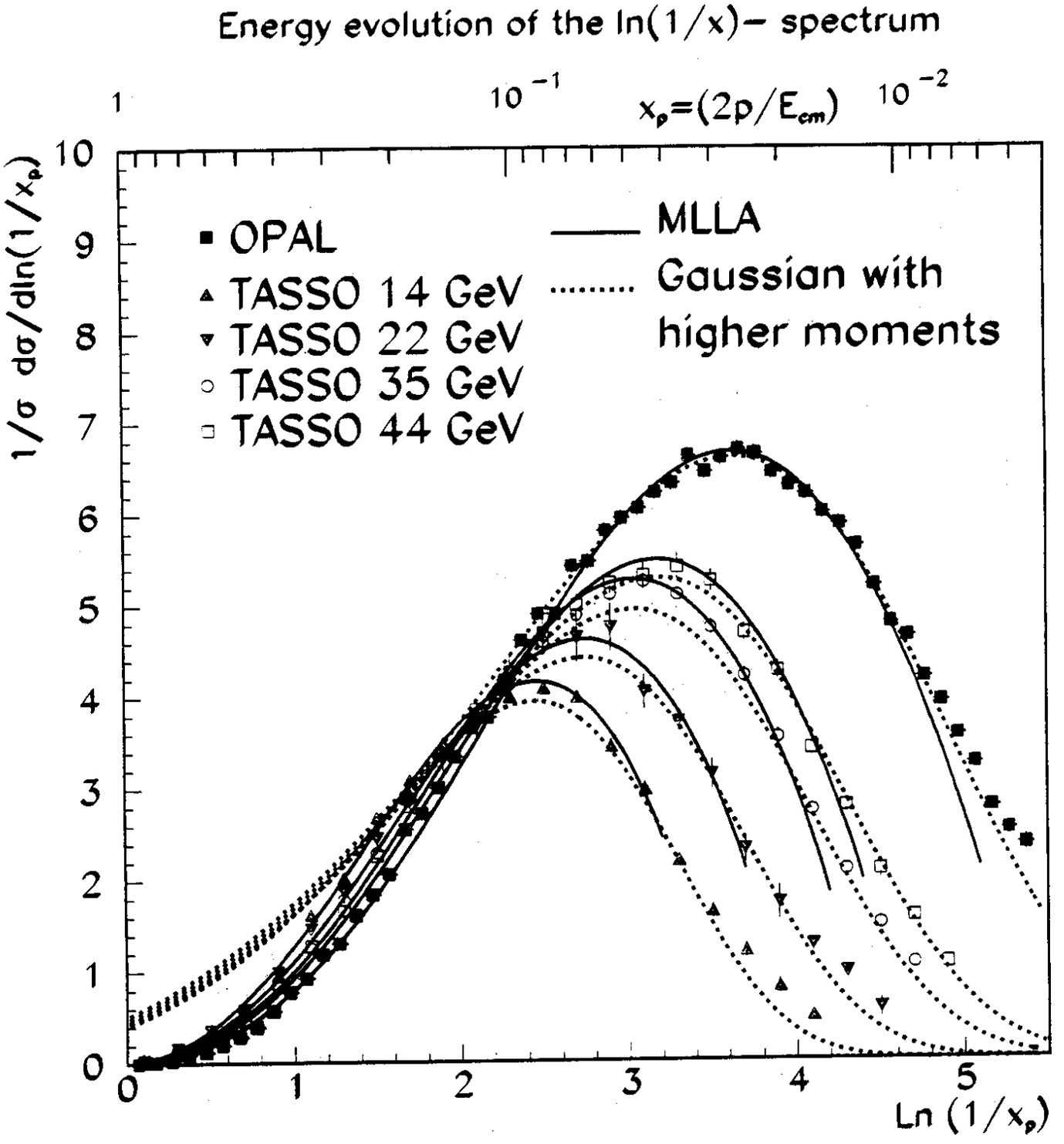
Energy evolution of the ln(1/x)– spectrum
1
10 -1
10 -2
x_p=(2p/E_cm)
1/σ dσ/dln(1/x_p)
OPAL
TASSO 14 GeV
TASSO 22 GeV
TASSO 35 GeV
TASSO 44 GeV
MLLA
Gaussian with higher moments
Ln (1/x_p)

Figure 3a

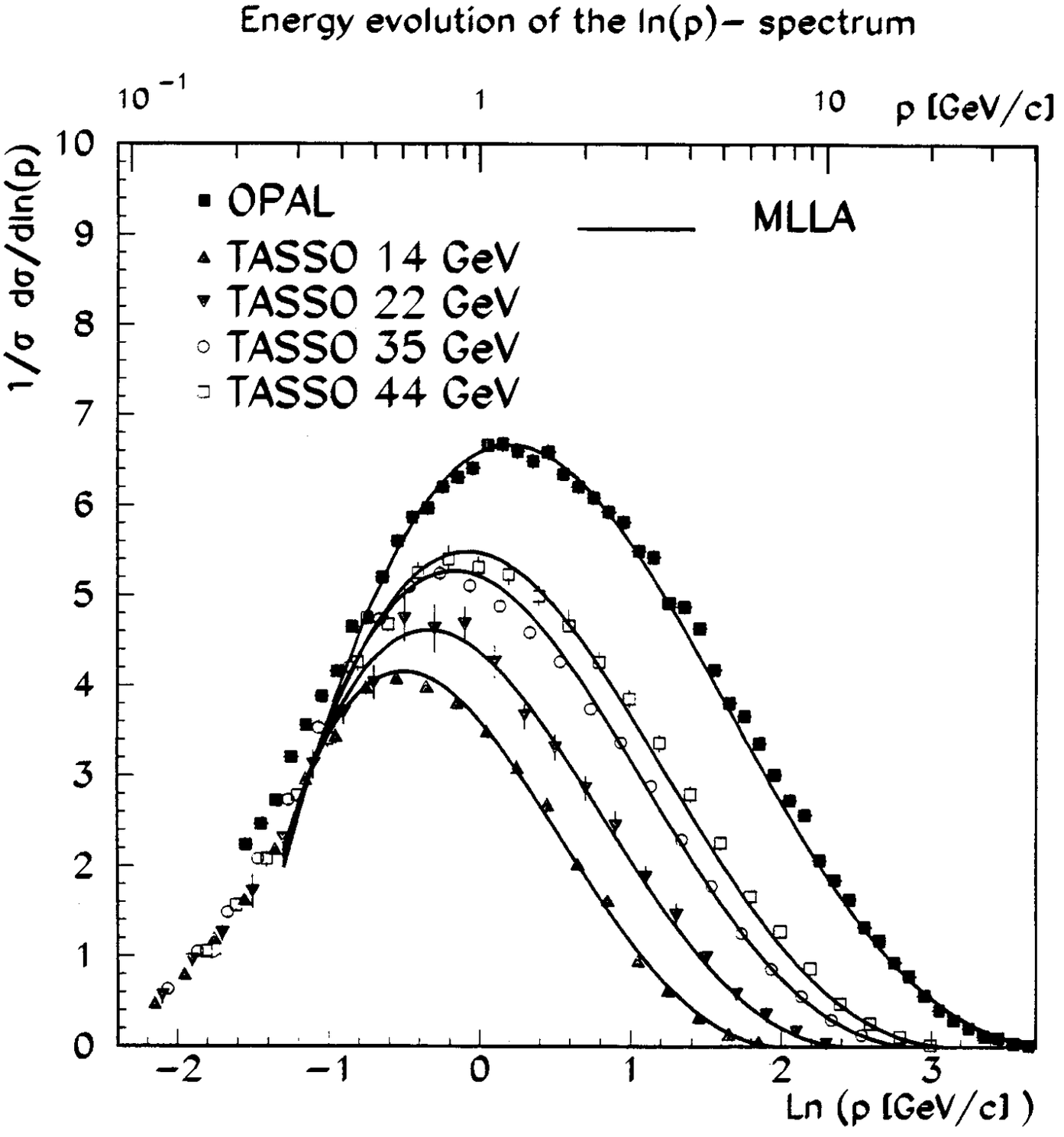
Energy evolution of the ln(p)– spectrum
10 -1
1
10
p [GeV/c]
1/σ dσ/dln(p)
OPAL
MLLA
TASSO 14 GeV
TASSO 22 GeV
TASSO 35 GeV
TASSO 44 GeV
Ln (p [GeV/c])

Figure 3b

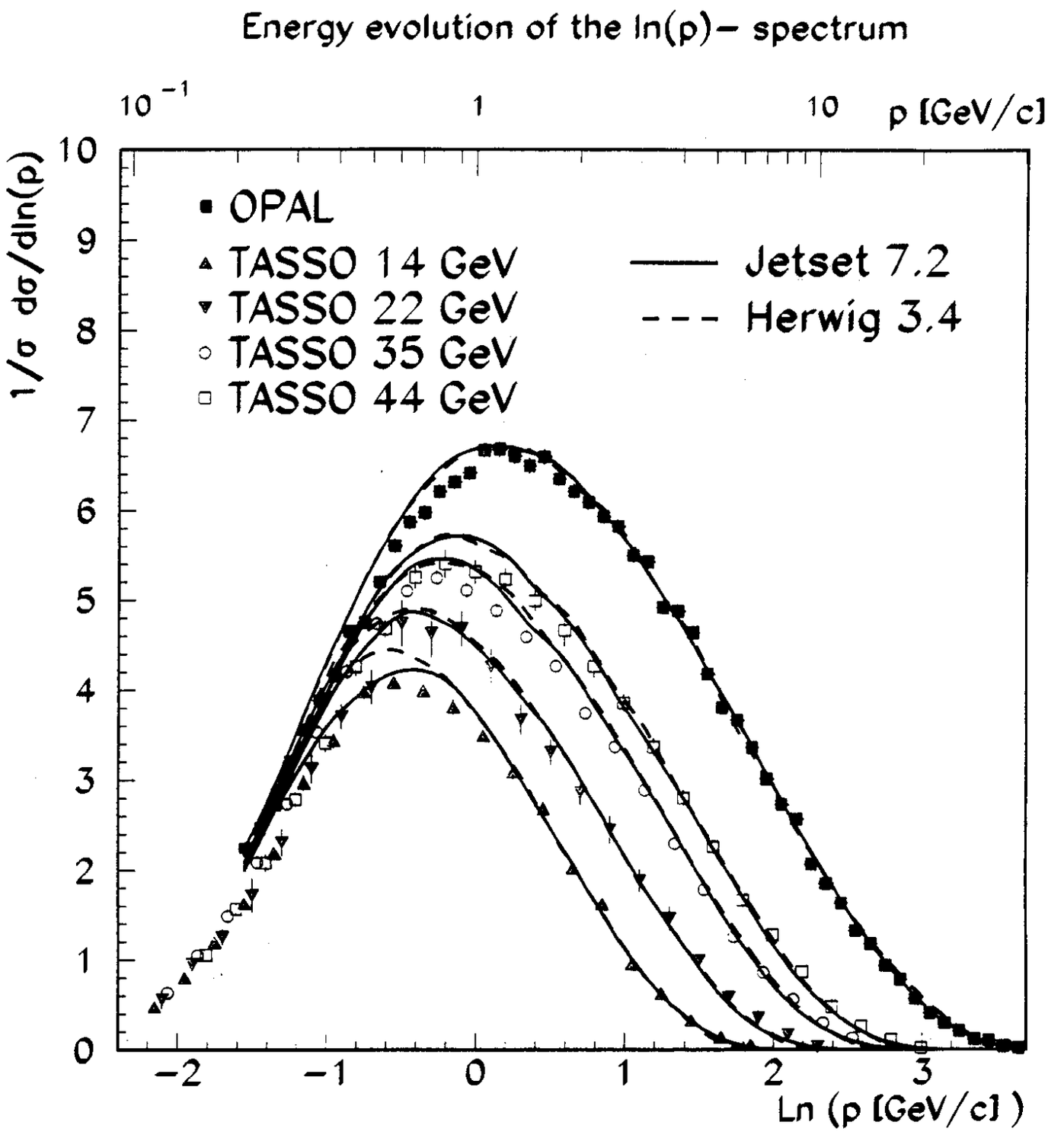
Energy evolution of the ln(p)– spectrum
10 -1
1
10
p [GeV/c]
1/σ dσ/dln(p)
OPAL
TASSO 14 GeV
TASSO 22 GeV
TASSO 35 GeV
TASSO 44 GeV
Jetset 7.2
Herwig 3.4
Ln (p [GeV/c])

Figure 3c

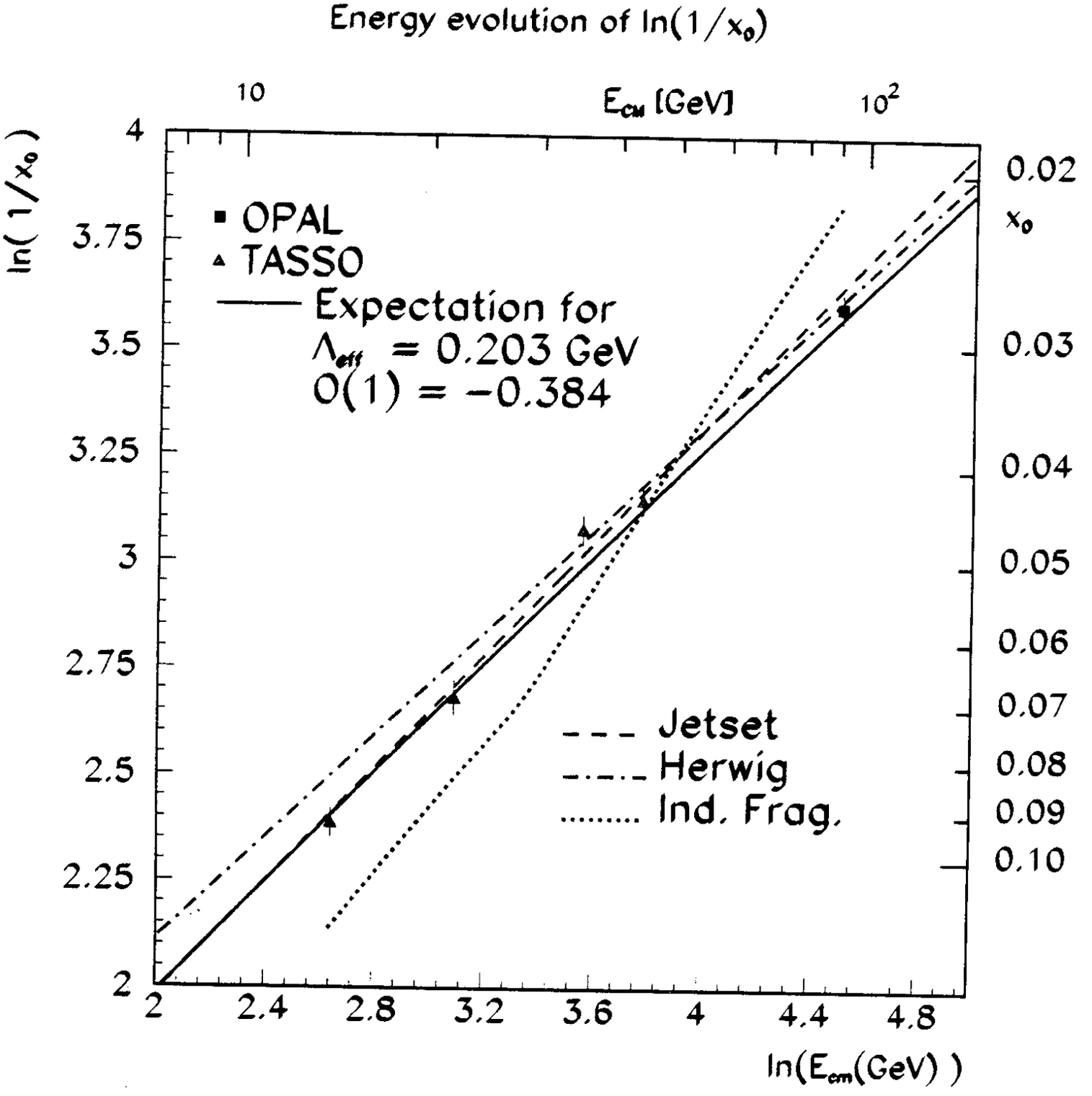

Figure 4

Imprimé au CERN. Prix : 0.65 Fr.